Current Science International
Volume: 15 | Issue: 03| July – Sept.| 2026

EISSN:2706-7920 ISSN: 2077-4435
DOI: 10.36632/csi/2026.15.3.13
Journal homepage: www.curresweb.com
Pages: 147-162

An Integrated Spatial Assessment Framework for Evaluating Flash Flood Hazard Potential in EL-Negila Coastal Area, Marsa Matruh Governorate, Western Desert, Egypt

Mona Y. Eldaly[1], Mohamed I. Al-Anbaawy[2], Mamdouh K. Abdel Ghaffar[1] and Tamer Nassar[2]

[1] Soil, Water and Environmental Research Institute, Agriculture Research Center, Giza, Egypt.
[2] Geology Department, Faculty of Science, Cairo University, Cairo, Egypt.

Received: 25 May 2026 **Accepted:** 20 June 2026 **Published:** 10 July 2026

ABSTRACT
The sustainable geo-environmental management of Egypt's El-Negila coastal region within the Marsa Matruh Governorate faces significant challenges, including the deterioration of natural resources driven by climate variability and flash flood occurrences. This research employs a multi-geospatial approach integrating satellite remote sensing data and GIS methodologies to map, monitor, and evaluate these environmental changes and associated hazards. Flash flood prediction maps were generated based on multiple factors encompassing topographic, meteorological, geological, and local conditions. A 30 m resolution Digital Elevation Model (DEM). This DEM served as the basis for extracting various topographic features, including elevation, slope, watershed characteristics (drainage density), and Topographic Wetness Index (TWI) within the GIS environment. LULC, NDVI, and road network data were derived from Sentinel-2 imagery acquired in 2025. Flash flood hazard evaluation utilized the multi-criteria Analytical Hierarchy Process (AHP) incorporating controlling parameters such as elevation, slope, watershed attributes (stream proximity and drainage density), LULC, normalized difference vegetation index (NDVI), road network proximity, topographic wetness index (TWI), lithological composition, and precipitation patterns. The resulting hazard zonation classified the region into three risk categories high, moderate, and low representing 33.78%, 63.06%, and 3.15% of the total area, respectively. The flood hazard map indicates that the most vulnerable zones are concentrated in the northern and eastern sectors, encompassing the tourism village, El-Negila town, and Marsa Matruh city. The mitigation strategies and management recommendations proposed in this investigation offer a practical framework for sustainable development planning in the region.

Keywords: Climate change, Flash flood hazards, Environmental mitigation procedures, El-Negaila coastal area.

1. Introduction

The study area represents one of Egypt's strategic development zones, with its prominence closely tied to agricultural activities, tourism potential, and urban expansion. Consequently, comprehensive spatial planning is essential to strengthen the region's resilience against both current and projected pressures, including population growth, industrial development, coastal resort construction, and the multifaceted impacts of climate change.

Effective geo-environmental stewardship of the El-Negaila coastal area in Egypt's Western Desert necessitates addressing challenges such as LULC transformations, shoreline erosion, flood vulnerability, and sustainable resource utilization. This encompasses understanding the complex interactions between wave dynamics, sediment transport, anthropogenic activities, and coastal

Corresponding Author: Mona Yousef Eldaly, 1 Soil, Water and Environmental Research Institute, Agriculture Research Center, Giza, Egypt.

morphology, while simultaneously formulating strategies for flood risk mitigation and sustainable development.

Floods constitute the most frequent, destructive, and lethal natural hazard globally (Malik and Pal 2021), accounting for approximately half of all-natural disaster-related fatalities over the past five decades and nearly one-third of worldwide economic losses.

Previous research worldwide has employed diverse decision-making and machine learning approaches to develop accurate flood susceptibility maps. Dou *et al*. (2017) applied the analytical hierarchy process with geospatial techniques to identify areas with high flood susceptibility. The AHP methodology represents a straightforward decision-support framework based on evaluating the relative significance of various contributing factors. Contemporary planning practitioners globally recognize the cost-effectiveness of GIS-based decision-support approaches for flood susceptibility zoning. The reliability of AHP outcomes depends substantially on the assigned factor weights. However, a noteworthy concern is the variation in weight assignments and rankings for specific parameters across different studies. Developing precise flood susceptibility maps requires careful consideration of data availability, accuracy, and regional contextual factors. Multi-criteria analysis (MCA)-based models are specifically designed to address complex multi-attribute problems such as flood assessment, integrating both qualitative and quantitative elements within decision-making frameworks (Dean, 2020). The integration of MCA methodologies with Geographic Information Systems (GIS) and Remote Sensing (RS) techniques has become standard practice, enabling comprehensive vulnerability assessment and identification of causative factors. This investigation employed the Analytical Hierarchy Process (AHP), recognized as one of the most established approaches for vulnerability evaluation (Aidinidou *et al*., 2023).

This study focuses on performing geo-environmental assessments of the El-Negaila coastal zone along Egypt's Mediterranean coast. Utilizing remote sensing (RS) and Geographic Information Systems (GIS), it employs the Flood Hazard Index (FHI) method to pinpoint the areas most susceptible to flooding.

Egypt is predominantly situated within arid climatic zones, characterized by dry conditions across most of its territory. However, the northwestern coastal belt experiences a subtropical Mediterranean climate featuring cool, wet winters and hot, arid summers. This coastal zone extends approximately 350 km from west of Alexandria to the Libyan border. Human settlements and land use patterns are heavily dependent on rainfall and various water harvesting techniques (Moustafa, 1994). Annual precipitation is confined to winter months and a narrow 20 km strip adjacent to the shoreline (Abdel-Kader and FitzSimon, 2002), decreasing rapidly with increasing distance from the coast. Rainfall patterns exhibit extreme irregularity, with substantial spatial variability both within and between years. Rainfall data spanning 64 years (1947-2010) were obtained from five meteorological stations distributed across northern Egypt, sourced from the Egyptian Meteorological Authority (2010) and www.tutiempo.net/clima (Table1). The Mediterranean climatic zone in northern Egypt experiences rainfall between October and April annually, with total annual amounts ranging from 100 to 220 mm, peaking in December or January. The study area's rainfall characteristics include sporadic occurrence, sudden onset, limited total volume, high intensity, and considerable interannual variability.

Table 1: Monthly distribution of annual rainfall at selected meteorological stations

	Total Rainfall												
Area	**Jan.**	**Feb.**	**Mar.**	**Apr.**	**May**	**Jun**	**Jul.**	**Aug.**	**Sep.**	**Oct.**	**Nov.**	**Dec.**	**Total /year**
Sallum	21	9.6	8.8	3.7	3.5	0.3	0	0.0	1.5	16	23.9	17.2	105.0
Sidi Barrani	46	14.6	15.6	6.7	3.4	0.1	0	0.0	0.8	22	22.2	40.0	171.4
Marsa Matruh	33	15.1	12.0	2.8	2.6	2.0	0	0.6	1.1	16	22.5	30.2	137.7
Ras El Hikma	43	9.8	11.7	5.7	0.9	0.1	0	0.0	3.4	15	20.8	37.0	147.1
El Dabaa	34	13.8	11.0	1.5	1.9	0.0	0	0.0	1.1	14	25.0	38.0	140.4

EISSN: 2706-7920 ISSN: 2077-4435 **DOI: 10.36632/csi/2026.15.3.13**

2. The Study Area

The El-Negila region is positioned along the northwestern coastal zone of Marsa Matruh Governorate, Egypt, situated between Matruh and Sidi Barani cities. It is bounded by the Mediterranean Sea to the north, coastal zones to the east and west, and the Western Desert to the south. The area extends between latitudes 31°29'36.815" to 31°7'50.232"N and longitudes 26°30'2.508" to 27°9'13.273"E show in (Figure 1), encompassing approximately 3169.44 km².

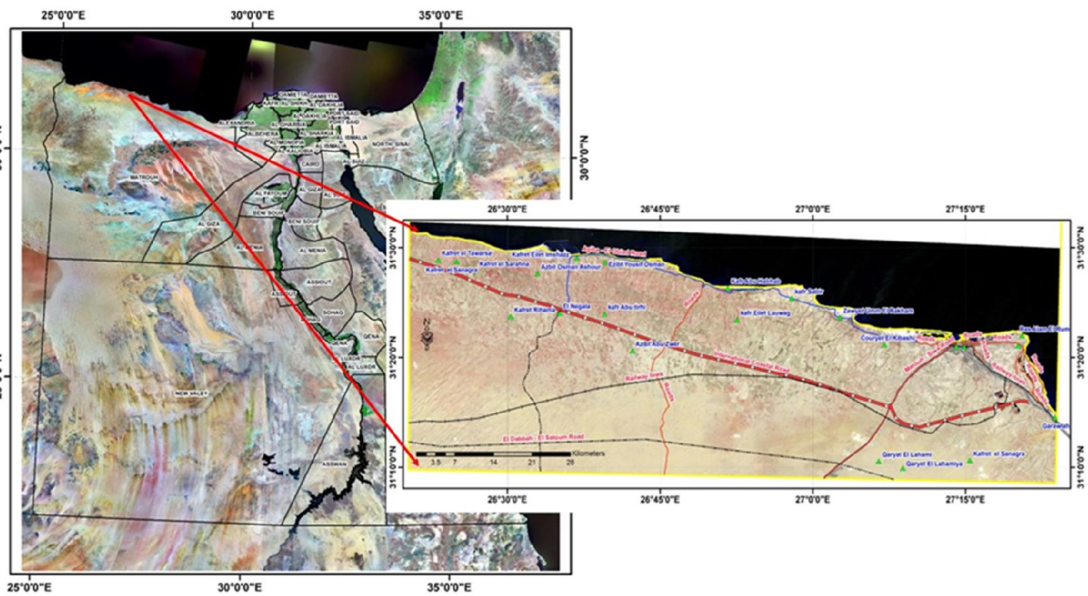

Fig. 1: Location map of the study area

Geologically the northern Western Desert comprises a predominantly featureless plain with few exceptions. Surface structures include several major fault lines and minor folds exhibiting gentle dips, while subsurface configurations display considerable complexity and intense tectonic activity. Most of the northern Western Desert is covered by a thin Miocene rock blanket unconformably overlying older strata. In the eastern sector, lower Miocene sediments rest upon basalt flows or Oligocene continental deposits, indicating a brief period of non-deposition and erosion. Toward the west, this unconformity truncates upper Eocene shales and marls (Said, 1961). According to the geological map (CONCO, 1987), exposed rock units from Marsa Matruh governorate to El-Gargoub Seaport range from Middle Miocene carbonates (Marmarica Formation) to Quaternary carbonates and clastics (Figure 2). In Marsa Matruh, Miocene sediments exhibit a major angular unconformity with Turonian dolomites (not exposed at the surface). The Miocene sequence terminates at an unconformity overlain by gently dipping coastal Pliocene sediments. The Middle Miocene Marmarica Formation displays the most extensive aerial distribution among the study area's rock units (Figure 2).

The primary objective was to screen 15 fungal isolates for production of dextranase, glucoamylase, and CMCase and to identify the most promising producers for subsequent characterization and optimization. A secondary objective was to explore the wider biotechnological value of the resulting isolate matrix, including industrial processing, agro-waste valorization, fermentation-feedstock development, and applications relevant to medical entomology.

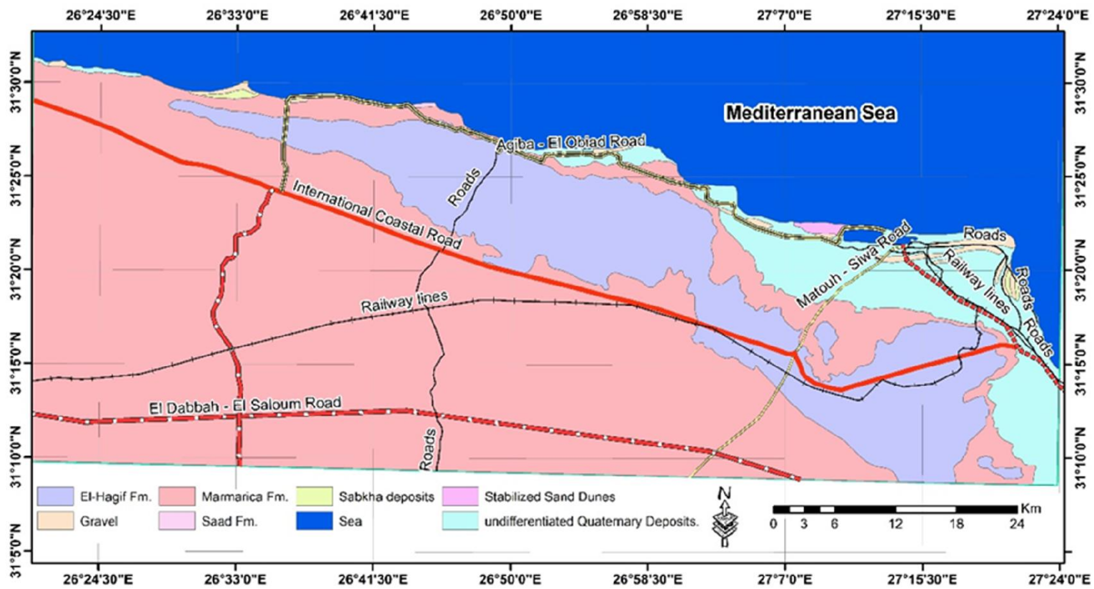

Fig. 2: Geologic map of the area between Marsa Matruh and El-Gargoub seaport modified after CONOCO, 1987).

2. Materials and Methods

3.1. Data used

Flash flood prediction maps were generated based on multiple factors encompassing topographic, meteorological, geological, and local conditions. A 30 m resolution Digital Elevation Model (DEM) was obtained from the United States Geological Survey (USGS) (https://earthexplorer.usgs.gov/). This DEM served as the basis for extracting various topographic features, including elevation, slope, watershed characteristics (drainage density), and Topographic Wetness Index (TWI) within the GIS environment. LULC, NDVI, and road network data were derived from Sentinel-2 imagery. (Table 2) provides a comprehensive breakdown of data sources. Prior to change detection analysis, classification accuracy was verified through field-based accuracy assessment procedures.

Table 2: Datasets utilized in the study

No.	Datasets	Description	Resolution /scale	Source
1	**Digital Elevation Model (DEM)**	SRTM (DEM)	30 m	USGS earth explorer https://earthexplrer.usgs.gov/
2	**Slope**	Derived from DEM	30 m	Same as DEM
3	**Topographic Wetness Index (TWI)**	SRTM (DEM)	30 m	Same as DEM
4	**Drainage Density**	Derived from DEM	30 m	Same as DEM
5	**Distance From Streams**	Derived from DEM	30 m	Same as DEM
6	**LULC**	Classification of Sentinal-2	10 m	Copernicus Browser https://browser.dataspace.copernicus.eu/
7	**NDVI**	Sentinal-2	10 m	Same as LULC
8	**Distance from roads**	Sentinal-2	10 m	Same as LULC
9	**Geology**	Geological map of Egypt	1:500000	CONOCO, 1987
10	**Rainfall**	Interpolation method in GIS	mm	Egyptian Meteorological Authority and www.tutiempo.net/clima

3.2. Flood Hazard Map:

The comprehensive methodology for flood hazard mapping is illustrated in Figure (3). The overall methodology for flood hazard mapping is as follows. First, a flood inventory and thematic maps representing all considered factors were created, including watershed parameters (drainage density and distance from streams), normalized difference vegetation index (NDVI), slope, land use/cover, rainfall, elevation, lithology, topographic wetness index, and distance to roads. Next, factors underwent multi-collinearity analysis to determine which flood-affecting factors should be included in model implementation. Analytical Hierarchy Process (AHP) was used to evaluate flood spatial relationships with different conditioning factors, involving weight assignment to systematically assess factor significance and impact, ultimately producing a flood prediction map in a GIS environment.

Flood hazard zone (FHZ) preparation was carried out in several steps: identifying and defining the complex problem, generating the AHP model-based hierarchical structure for selected criteria, performing pairwise comparison matrix analysis for chosen influencing variables, assessing priority values and determining relative weights, measuring consistency values for evaluations, and synthesizing conclusions on priority variables to identify FHZ (Danumah *et al*., 2016; Roy and Blaschke, 2015). Influencing factors were further reclassified into sub-classes according to relative ranks for computation of relative weights (Danumah *et al*., 2016; De Brito and Evers, 2016).

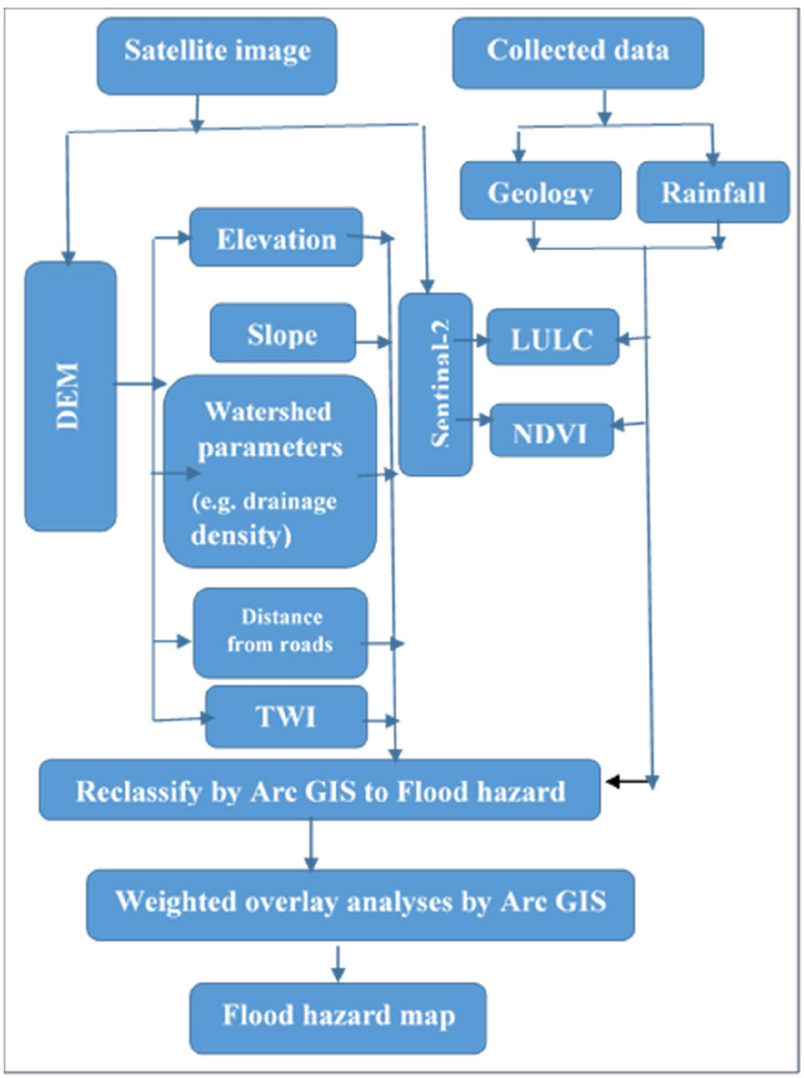

Fig. 3: Methodology flow chart of flood hazard map

4. Results and Discussion

4.1. Analytical Hierarchy Process (AHP) for Relative Weightage

Factor weights applied in the study area were determined using AHP (Saaty, 1980; Dou *et al*., 2017). The AHP methodology constitutes a mathematical approach for characterizing complex problems with varying numbers of factors. Once all factors were hierarchically arranged, a pairwise comparison matrix was constructed to enable meaningful assessment comparisons. The relative importance of each factor was determined using nine numerical scales, as shown in (Table 3).

Table 3: Numerical expression of the relative importance of factors (Saaty scale 1980).

Importance	Numerical scale	Reciprocal
Equally Important	1	1
Equally to Moderately Important	2	1/2
Moderately Important	3	1/3
Moderately to Strongly Important	4	1/4
Strongly Important	5	1/5
Strongly to Very Strongly Important	6	1/6
Very Strongly Important	7	1/7
Very Strongly to Extremely Important	8	1/8
Extremely Important	9	1/9

Following completion of all pairwise comparisons, the principal eigenvector of the matrix was calculated to derive relative weights for each factor. This process involved normalizing the comparison matrix by dividing each element by its column total, then calculating the average of each row in the normalized matrix. The resulting eigenvector represents the relative weights of each factor in the flood susceptibility model. Relative weights were calculated by deriving the principal eigenvector of a 10 × 10 square reciprocal matrix, with criteria ratings estimated through expert judgment and literature review using the nine-point continuous scale (Saaty 1980), as shown in (Table 3).

4.2. Watershed characteristics:

The study area represents a part of the coastal desert downstream zone including structurally controlled paleo-drainage wadi channels (Figure.4). Many hydrologic basins were delineated with their water points and stream ordering (Figure.4). Several morphometric parameters were determined based on watershed analysis. Some of these parameters control flash flood hazards potentially in the area, of which stream order, steam length, basin relief, shape and dimensions as well as drainage density. The stream ordering (linear aspect) designate the relative position of stream segments in an erosional drainage network. The stream ordering level Seam to be attributed to variation of basin dimension as well as slope, physiographic structure and infiltration capacity within the basin.

The basins generally exhibit dendritic patterns and elongated shapes trending perpendicular to the Mediterranean shoreline (Figure 4). They are characterized by low relief and gentle slopes, resulting in moderate drainage density and coarse basin texture with relatively permeable sub-soil, particularly within scattered sand sheet areas. During heavy rainstorm periods, runoff water accumulates at minor wadi outlet points where each stream segment joins higher order streams, creating water points. Accumulated water follows the general northern and northeastern wadi channels toward the lowest sites of major water points near the Mediterranean shoreline (Figure 4).

Although arid, the study basins are crucial for local water resources, primarily supplied by winter rainfall. The drainage characteristics of basin terrain surfaces required for flash flood risk assessment indicate significant potential for receiving flash floods with peak runoff due to the weathered and fractured nature of the Marmarica plateau bedrock (Morad *et al*., 2014).

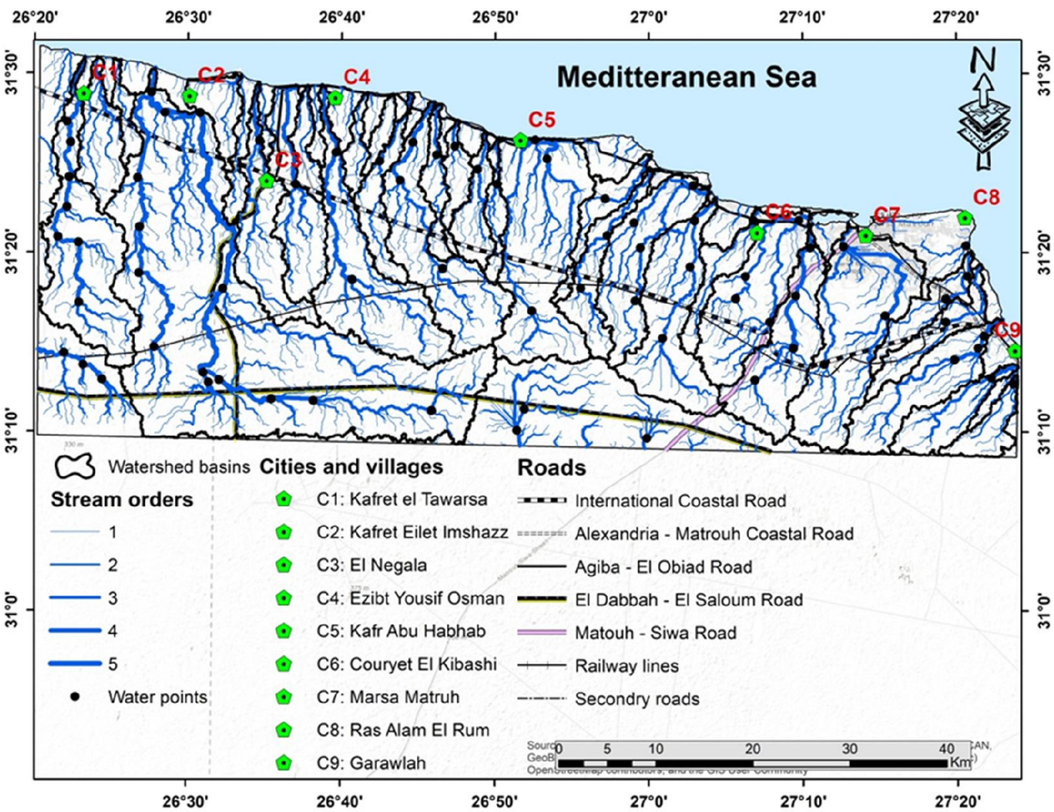

Fig. 4: Watershed basins, stream orders and water points of the study area

4.3. Flood Hazard Index (FHI) Factors:

The factors incorporated in the spatial flood map were extracted from the 30 m × 30 m resolution DEM, including elevation, TWI, slope, drainage density, and stream distance. The rainfall spatial distribution map was derived from regional extrapolation incorporating five meteorological stations bordering the study area (see Table 1). LULC, NDVI, and road networks were obtained from Sentinel-2 satellite imagery of the area. All information was organized in a database using ArcGIS software 10.8.

Elevation (DEM): In flood hazard mapping, elevation is considered the most critical factor controlling flood vulnerability according to expert opinion (Mojaddadi *et al*. 2017). Higher elevations generally exhibit lower flood potential, whereas lower elevations have higher vulnerability. Water tends to flow from higher to lower regions; therefore, low- elevation areas with flat surfaces have greater flood occurrence potential (Das *et al*., 2018). Elevation within the study area ranges from 0 m to 204 m above mean sea level (m a.s.l.), (Table 4 and Figure 5).

Topographic Wetness Index (TWI): (TWI) indicates the effect of Topography on Runoff Generation and the amount of flow accumulation at any location in river catchments (Gokceoglu *et al*., 2005). TWI is computed using an equation:

TWI = ln (Specific Catchment Area / tan (slope))
where Specific Catchment Area = (Catchment Area/Unit Contour Length)
Catchment Area = (Flow Accumulation Raster + 1) × (Area of each cell)
tan (slope) = (Slope Raster/100) + 0.001

Flow accumulation raster and slope (percent rise) were used as input in the raster calculator tool of ArcGIS 10.8 to generate TWI maps. The TWI for the study area ranges from 4.1 to 24.0 m^2 (Table 4, Figure 5).

Distance from Streams (DFS): Spatial distance to the stream system is a crucial factor in flood vulnerability zone delimitation. As distance to the stream system decreases, flood risk increases (Kazakis *et al*., 2015). Distances below 1030 m to the stream system correspond to areas of higher flood vulnerability, while areas located beyond 5170 m from the stream system present lower or absent flood risk. High flood vulnerability zones are mainly confined to stream networks (Table 4, Figure 5).

Drainage Density (DD): Drainage density serves as a key metric for assessing watershed behavior affecting water flow, flood risk, and erosion potential. It is defined as total stream length per unit area (km/km^2). Regions with higher drainage density exhibit increased surface runoff, elevating flood likelihood (Vojtek and Vojteková, 2019). In this study, a flow accumulation raster generated from the DEM served as input for the line density analysis tool in ArcGIS to create a drainage density map. In the study catchment, DD values range from 0 to 6.51 m/km^2, with the lower class concentrated in the catchment (Table 4, Figure 5).

Rainfall (R): Rainfall is the most important factor related to flood occurrence for a given area, having a direct relationship with stream flow; large rainfall amounts in short periods can generate flash floods in semi-arid regions (Abdulrazzak *et al*., 2019). A rainfall map was prepared from annual mean rainfall by inverse distance weighted (IDW) interpolation in ArcGIS 10.8 (Yoo *et al*., 2021). Annual mean rainfall varies between 118.0 and 138.0 mm/year (Table 4, Figure 5).

Slope (S): Surface slope plays a vital role in flood susceptibility. Gentle slope regions are more vulnerable to flooding due to water retention, while steeper slopes are less affected as water drains rapidly downslope (Chen *et al*., 2015). A slope gradient map was created using the DEM and slope function tool in ArcGIS, ranging from 0° to 32.4° (Table 4, Figure 5).

Land use / Land cover (LULC): The type and distribution of various LULC categories critically influence flood likelihood and intensity. Flood mechanisms vary with land use categories such as urban areas, vegetated regions, and areas with soil or rocky textures (Farhadi and Najafzadeh, 2021). Agriculture generally favors infiltration through root systems, whereas built-up areas reduce infiltration and increase surface runoff. Land use data were reclassified into six classes displayed in the Figure, then further reclassified into five classes based on weights (Table 4, Figure 5).

Normalized Difference vegetation index (NDVI): NDVI values range from -1 to 1, where negative values correspond to water, near-zero values indicate bare soil or rocks, and higher values reflect dense, healthy vegetation (Soltani *et al*., 2021). The NDVI map was prepared from a Sentinel-2 satellite image and calculated from the following equation:

$$NDVI = (NIR - RED) / (NIR + RED)$$

NDVI has a negative relationship with flooding: higher NDVI values indicate lower flood

probability, while lower NDVI values indicate higher flood probability. In this study, NDVI values range from -0.30 to 0.63 and were classified into five classes using the natural breaks method (Table 4, Figure 5).

Distance from Road: Distance from roads is also important in quantifying flood vulnerability. During floods, water flowing over stream banks floods low-lying areas, entering roads and streams and damaging public properties, roads, and houses. In this study, distance from roads is classified into five classes from very high (0 - 1300 m) to very low (7101 - 12000 m) (Table 4, Figure 5).

Geology: The geological variations in a region can significantly alter the profile of a wadi due to temporal floods (Reneau, 2000), making this a key factor in increasing the severity of flood events. Furthermore, the geology of an area can offer crucial insights into the frequency of past flood occurrences (He *et al*., 2007). There is a strong correlation between a rock's infiltration rate and its permeability (Table. 4). In the study area, the Marmarica and Hagif formations are characterized by highly impermeable rock, leading to low infiltration rates, which indicates a high risk of flooding. In contrast, the Quaternary deposits consist of rocks with low impermeability and high infiltration rates, suggesting a lower flood risk.

Table 4: Weights of sub-classes using AHP comparison matrix.

Flood Causative Criterion	Units	Class	Susceptibility class ranges and ratings	Susceptibility class ratings
TWI	Level	4.1 - 7.6	Very Low	1
		7.7 - 9.7	Low	2
		9.8 - 12	Moderate	3
		13 - 15	High	4
		16 - 24	Very High	5
Elevation	m	0 - 42	Very High	5
		42.1 - 86	High	4
		86.1 - 126	Moderate	3
		127 - 158	Low	2
		159 - 204	Very low	1
Slope	(Degree)	0 - 0.89	Very High	5
		0.891 - 2.29	High	4
		2.3 - 4.32	Moderate	3
		4.33 - 8.77	Low	2
		8.78 - 32.4	Very low	1
Precipitation	mm/year	118 - 123	Very Low	1
		124 - 127	Low	2
		128 - 131	Moderate	3
		132 - 135	High	4
		136 - 138	Very High	5
LULC	Level	Water Bodies	Very High	5
		Built up	High	4
		Barren land	Moderate	3
		Shore / beach deposits	Low	2
		Agriculture and Natural Plants	Very Low	1
NDVI	Level	-0.3 – 0.046	Very High	5
		0.046 – 0.18	High	4
		0.19 – 0.28	Moderate	3
		0.29 - 0.38	Low	2
		0.39 – 0.63	Very Low	1
Distance From Streams	m	0 - 1,030	Very High	5
		1,040 - 2,070	High	4
		2,080 - 3,100	Moderate	3
		3,110 - 4,140	Low	2
		4,150 - 5,170	Very Low	1
Geology	Level	Marmarica Fm.	Very High	5
		El-Hagif Fm./Saad Fm.	High	4
		Undifferentiated Quaternary and Sabkha deposits	Moderate	3
		Gravel	Low	2
		Stabilized Sand Dunes	Very Low	1
Drainage Density	km/km^2	0 - 1.3	Very Low	1
		1.31 - 2.6	Low	2
		2.61 - 3.91	Moderate	3
		3.92 - 5.21	High	4
		5.22 - 6.51	Very High	5
Distance From Roads	m	0-1300	Very High	5
		1301-2700	High	4
		2701-4500	Moderate	3
		4501-7100	Low	2
		7101-12000	Very Low	1

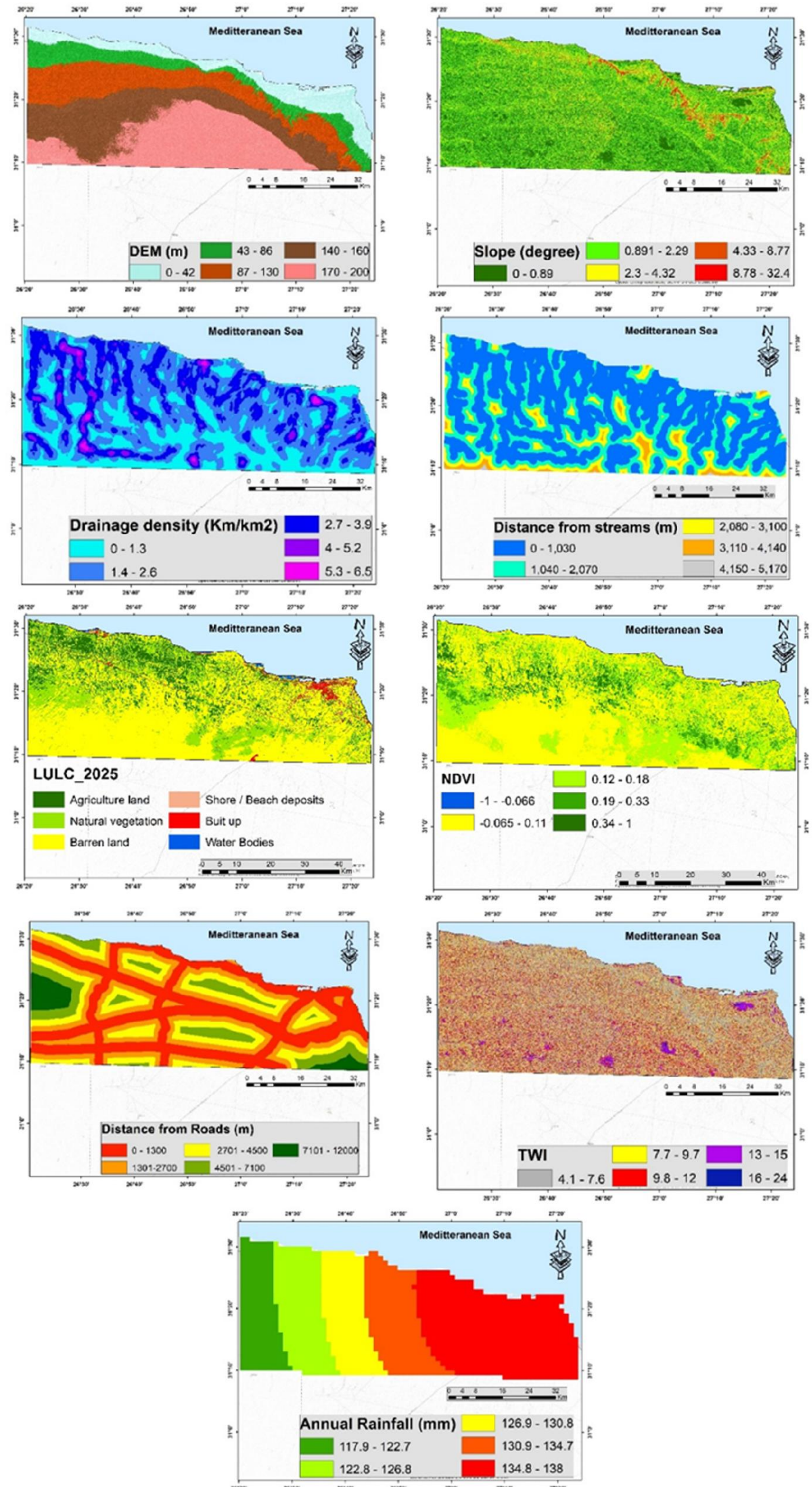

Fig. 5: Controlling factors of flood hazard in the study area: (a) DEM, (b) Slope, (c) Drainage density, (d) Distance from streams, (e) LULC, (f) NDVI, (g) distance from roads, (h) TWI, (i) Annual rainfall.

Curr. Sci. Int., 15(3): 147-162, 2026
EISSN: 2706-7920 ISSN: 2077-4435 **DOI: 10.36632/csi/2026.15.3.13**

Table 5: Pairwise comparison matrix of flood influencing factors for AHP

Matrix	TWI	Elevation	Slope	Precipitation	LULC	NDVI	Distance from streams	Hillshade	Drainage density	Geology	Relative weights
TWI	1	1	1	1	3	5	1	3	1	1	13.48
Elevation	1	1	1	1	2	3	1	3	1	1	11.99
Slope	1	1	1	1	3	1	1/2	1	1	1	9.98
Precipitation	1	1	1	1	3	2	2	3	1	1	13.25
LULC	1/3	1/2	1/3	1/3	1	1	1/3	3	1	1	6.70
NDVI	1/5	1/3	1	1/2	1	1	1/5	1	1	1	6.04
Distance from streams	1	1	2	1/2	3	5	1	3	1	1	13.85
Distance from roads	1/3	1/3	1	1/3	1/3	1	1/3	1	1	1	5.74
Drainage density	1	1	1	1	1	1	1	1	1	1	9.48
Geology	1	1	1	1	1	1	1	1	1	1	9.48
Total	7.86	8.16	10.33	7.66	18.33	21.00	8.36	20.00	10.00	10.00	100.0

4.5. Spatial Distribution of Flood hazard

The flood hazard map for the study area was generated by overlaying thematic maps of different flood conditioning factors, using relative weights obtained from AHP in a weighted overlay analysis within ArcGIS, as outlined in (Table 5). The flood hazard map was classified into three distinct categories: low, moderate, and high hazards (Table 6 and Fig. 6). The respective areas corresponding to different degrees of flood risk varied: 33.78% (high risk), 63.06% (moderate risk), and 3.15% (low risk) (Table 6). Most high flood risk areas are concentrated near drainage lines (streams) and in the northern and eastern parts of the study area. Notably, this zone includes many urban areas with significant infrastructure and population, such as Marsa Matrouh city, tourism village, and El-Negila city. These vulnerable zones are characterized by low elevation, gentle slopes, and increased drainage density, aligning with findings from multiple studies (Vojtek and Vojtekova, 2019; Varra *et al*., 2024; Nguyen *et al*., 2024). This situation underscores the critical need for comprehensive flood mitigation strategies in these areas. The central portion of the study area, with its moderate elevation, low slope, and developed land use, predominantly falls within the moderate flood hazard category. Meanwhile, the southwestern sections, showing higher elevations, steeper slopes, greater distance from streams, and barren land cover, exhibit low flood hazard.

Table 6: Area coverage of different flood hazard classes.

Flood hazard classes	Area (km^2)	Percentage (%)
High	1070.77	33.78
Moderate	1998.75	63.06
Low	99.92	3.15
Total	3169.44	100.00

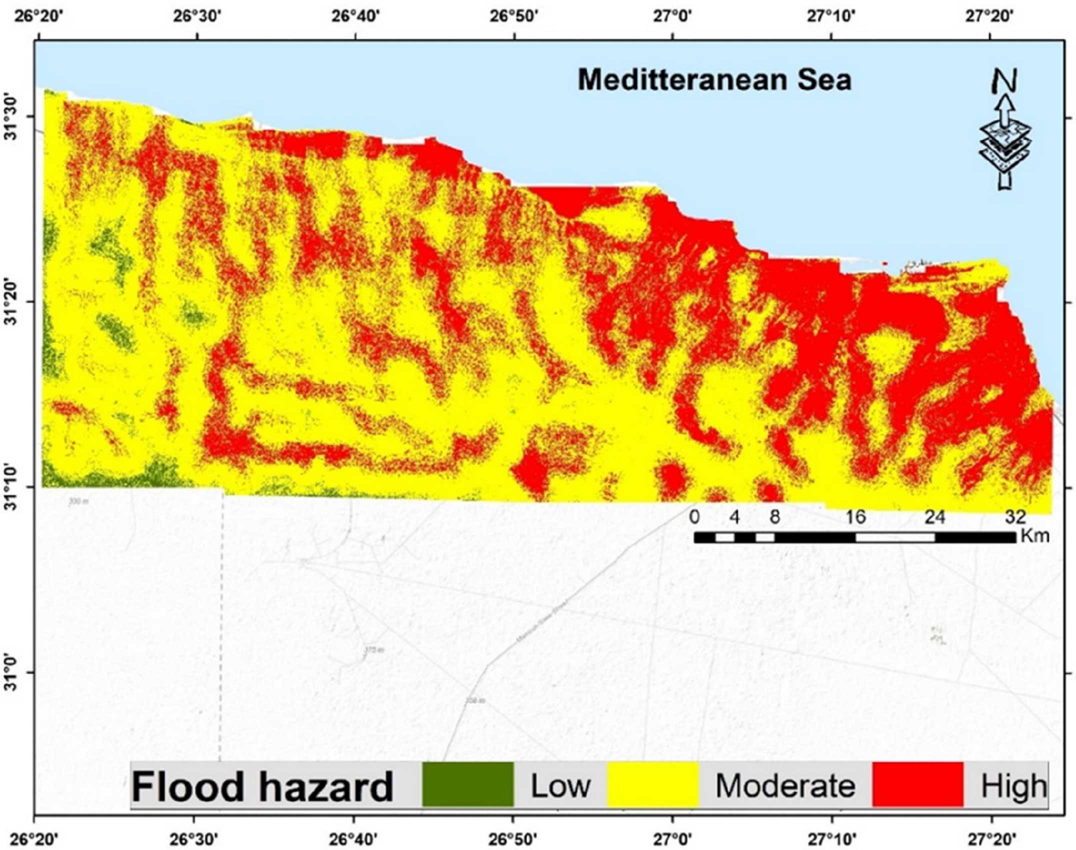

Fig. 6: Flood hazard map of El-Negila Coastal area

The flood in October 2023

The flood in October 2023, marking the first catastrophic event of this kind in the recorded history of Matruh Governorate, came unexpectedly. It was caused by severe thunderstorms linked to Storm Daniel over the area. Historically, this region has not experienced significant flooding, highlighting its increasing vulnerability to extreme weather events, likely worsened by climate change (Ezz, 2025). The worst-hit areas included Wadi Al-Raml, Al-Kharouba, and Kilo 4, where heavy rainwater led to extensive pooling (Figure 7).

Fig. 7: Photos of flood in Marsa Matruh city at Oct. 2023

4.6. Flood Mitigation for Sustainable Development

Based on field investigation and hydrological study, flash flood mitigation measures were designed. Potential water harvesting sites were examined considering different land slopes, topography, land use, permeability, and physical characteristics (potential water). Subsequently, physical and social factors were combined in the site selection process (Kamel, 2022).

Existing dams:

Field investigations indicated that an earth fill dam exists on the upstream side of the floodwater direction, with gradual height ranging from 1.0 m to 3.0 m maximum (Figure 8). The field investigations also indicated six diversion dams along the wadi channel, perpendicular to the floodwater direction. Due to sedimentation (siltation) from successive storms, the existing dams lost their function due to the huge accumulated sediments in front of them.

Fig. 8: Exiting dams across wadi channels in the study area

Proposing mitigation (protection) measures:

The needs of residents are to be protected from flash flood dangers, in addition to their desire to make the most of that water for agricultural activities. Consequently, the second alternative for flood mitigation was chosen: proposing structural measures to control floods in the downstream of the basins. This alternative consists of two main parts: upgrading existing structures and proposing new measures (Figure 9). Consequently, all structures could work together for water harvesting purposes and reducing flood risks.

These measures include:

- Culvert installation under main roads crossing major streams to facilitate safe passage of runoff water.
- Pits or pond excavation at water point locations to accumulate excess runoff water during heavy rainfall events and consequently recharge the shallow alluvium aquifer.
- Additional protective systems, such as construction of sandy and gravel barriers along broad channels within water point locations to reduce water velocity and enhance groundwater recharge.
- Selection of measure type depends on the geomorphological condition near or within the water point location (Figure 9).

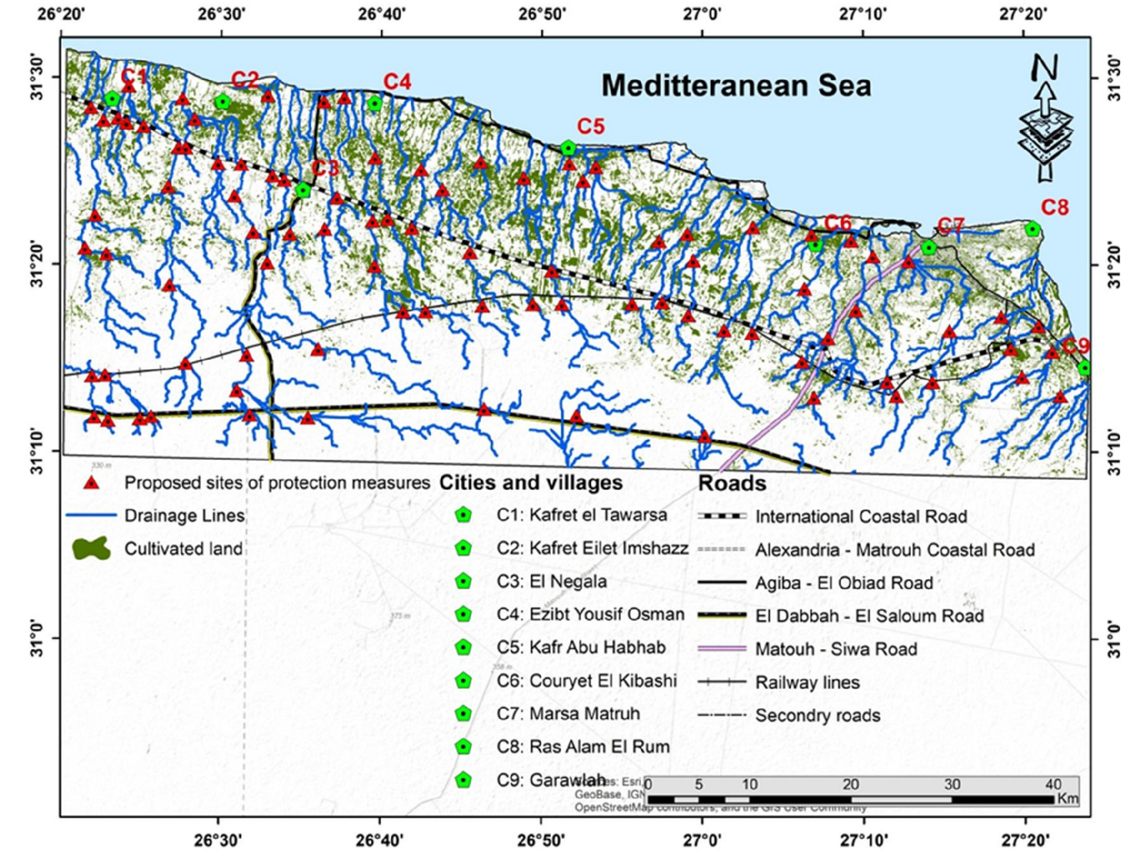

Fig. 9: Location of proposed sites of protection measures in the study area

5. Conclusions and Recommendation

The flood hazard map was classified into three distinct categories: low, moderate, and high hazards. Most high flood risk areas are concentrated near drainage lines (streams) and in the northern and eastern parts of the study area. It is essential to note that this zone encompasses numerous urban areas with substantial infrastructure and population, including Marsa Matruh city, the tourism village, and El-Negila city. These vulnerable zones are characterized by low elevation, gentle slopes, and increased drainage density.

Based on physical and social factors, flash flood mitigation measures were designed to satisfy the needs of built-up areas. Additional protective measures were proposed, such as: culvert installation, excavated pits/ponds, and gravelly barriers in the downstream of the basin for reducing flood risks and water harvesting purposes.

The findings of this paper can assist managers and decision-makers in their future development plans in the study area. In case of implementing the proposed mitigation measures, the harvested stormwater would promote expansion activities and create an appropriate climate for implementation of development plans in the area.

References

Abdel-Kader, F. H., and J. FitzSimon, 2002. Participatory land and water management in dryland agropastoral areas. NW Coast of Egypt. Final Report, Department of Soil and Water Sciences, Faculty of Agriculture, Univ. of Alexandria, Egypt.

Abdulrazzak, M., A. Elfeki, A. Kamis, M. Kassab, N. Alamri, A. Chaabani and K. Noor, 2019. Flash flood risk assessment in urban arid environment: case study of Taibah and Islamic universities' campuses, Medina, Kingdom of Saudi Arabia. Geomatics, Natural Hazards and Risk, 10(1), 780–796. https://doi.org/10.1080/19475705.2018.1545705

Aidinidou, M. T., K. Kaparis and A. C. Georgiou, 2023. Analysis, prioritization and strategic planning of flood mitigation projects based on sustainability dimensions and a spatial/value AHP-GIS system, Expert Systems with Applications, 211,118566. https://doi.org/10.1016/j.eswa.2022.118566.

Chen, Y., R. Liu, D. Barrett, L. Gao, M. Zhou, L. Renzullo and I. Emelyanova, 2015. A spatial assessment framework for evaluating flood risk under extreme climates. Sci Total Environ., 15;538:512-23. doi: 10.1016/j.scitotenv.2015.08.094.

CONOCO, 1987 Geological Maps of Egypt Scale 1:500,000. Sheet Nos. NG 36 NW Cairo, The Egyptian General Petroleum Corporation, Egypt.

Danumah, J.H., S.N. Odai and B.M. Saley, *et al.,* 2016. Flood risk assessment and mapping in Abidjan district using multi-criteria analysis (AHP) model and geoinformation techniques, (cote d'ivoire). Geoenviron Disasters 3, 10. https://doi.org/10.1186/s40677-016-0044-y

Das, S., S.D. Pardeshi and P.P. Kulkarni, *et al.,* 2018. Extraction of lineaments from different azimuth angles using geospatial techniques: a case study of Pravara basin, Maharashtra, India. Arab J Geosci., 11, 160. https://doi.org/10.1007/s12517-018-3522-6.

de Brito, M.M. and M. Evers, 2016. Multi-criteria decision-making for flood risk management: a survey of the current state of the art, Nat. Hazards Earth Syst. Sci., 16, 1019–1033. https://doi.org/10.5194/nhess-16-1019-2016.

Dean, M., 2020. Multi-criteria analysis. In book: Standard Transport Appraisal Methods. (Advances in Transport Policy and Planning; Vol. 6). Academic Press. DOI: 10.1016/bs.atpp.2020.07.001.

Dou, X., Song, J., Wang, L. *et al.* Flood risk assessment and mapping based on a modified multi-parameter flood hazard index model in the Guanzhong Urban Area, China. Stoch Environ Res Risk Assess, 32, 1131–1146 (2018). https://doi.org/10.1007/s00477-017-1429-5

Egyptian Meteorological Authority, 2010. Rainfall and temperature data for meteorological stations in Egypt.

Ezz, H., 2025. Unexpected Flooding In Mersa Matruh, Egypt investigating Causes, Hydrological Analysis, and Flood Risk Assessment. Larhyss Journal, n°61, March 2025, pp. 371-399

Farhadi, H., and M. Najafzadeh, 2021. Flood Risk Mapping by Remote Sensing Data and Random Forest Technique. Water*,* 13(21), 3115. https://doi.org/10.3390/w13213115.

Gokceoglu, C., H. Sonmez, H. A. Nefeslioglu, T. Y. Duman and T. Can, 2005. The 17 March 2005 Kuzulu landslide (Sivas, Turkey) and landslide-susceptibility map of its near vicinity, Engineering Geology, 81(1): 65-83. https://doi.org/10.1016/j.enggeo.2005.07.011.

He, B., Yi-Gang Xu, Xiao-Long Huang, Zhen-Yu Luo, Yu-Ruo Shi, Qi-Jun Yang, Song-Yue Yu, 2007. Age and duration of the Emeishan flood volcanism, SW China: Geochemistry and SHRIMP zircon U–Pb dating of silicic ignimbrites, post-volcanic Xuanwei Formation and clay tuff at the Chaotian section, Earth and Planetary Science Letters. 255(3–4):306-323. https://doi.org/10.1016/j.epsl.2006.12.021.

Kamel, A. M., 2022. Flash Flood Mitigation for Sustainable Development in Arid Regions. Contingency Planning of Adaptive Urbanism. DOI: 10.21608/furp2022.2022.1815.

Kazakis, N., I. Kougias and T. Patsialis, 2015. Assessment of flood hazard areas at a regional scale using an index-based approach and Analytical Hierarchy Process: Application in Rhodope–Evros region, Greece, Science of The Total Environment, 538555-563. https://doi.org/10.1016/j.scitotenv.2015.08.055

Malik, S. and S.C. Pal, 2021. Potential flood frequency analysis and susceptibility mapping using CMIP5 of MIROC5 and HEC-RAS model: a case study of lower Dwarkeswar River, Eastern India. SN Appl. Sci. 3, 31. https://doi.org/10.1007/s42452-020-04104-z.

Mojaddadi, H., B. Pradhan, H. Nampak, N. Ahmad and A. bin Ghazali, 2017. Ensemble machine-learning-based geospatial approach for flood risk assessment using multi-sensor remote-sensing data and GIS. Geomatics. Natural Hazards and Risk, 8(2), 1080–1102. https://doi.org/10.1080/19475705.2017.1294113.

Morad, N.A., M.H. Masoud, and S.M.A. Moghith, 2014. Hydrologic factors controlling groundwater salinity in northwestern coastal zone, Egypt. J Earth Syst Sci., 123, 1567–1578. https://doi.org/10.1007/s12040-014-0483-3.

Moustafa, A.T.A., 1994. Agriculture Development in the Northwestern Zones of Egypt. In: FAO. 1994. Water Harvesting for Improved Agricultural Production: Proceedings of the FAO Expert Consultation, Cairo, Egypt 21-25 November 1993. FAO Water Reports 3. Rome.

Nguyen, H.N., H. Fukuda and M.N. Nguyen, 2024. Assessment of the Susceptibility of Urban Flooding Using GIS with an Analytical Hierarchy Process in Hanoi, Vietnam. Sustainability, 16(10): 3934. https://doi.org/10.3390/su16103934.

Roy, D. C., and T. Blaschke, 2015. Spatial vulnerability assessment of floods in the coastal regions of Bangladesh. Geomatics, Natural Hazards and Risk, 6(1): 21–44. https://doi.org/10.1080/19475705.2013.816785

Saaty, T. L., 1980. The Analytic Hierarchy Process; Golden, B.L., Wasil, E.A., Harker, P.T., Eds.; Springer: Berlin/Heidelberg, Germany, 1980.

Said, R., 1962. Geology of Egypt. Elsevier Publ. Co., Amsterdam and New York, 293-319.

Soltani K., I. Ebtehaj, A. Amiri, A. Azari, B. Gharabaghi and H. Bonakdari, 2021. Mapping the spatial and temporal variability of flood susceptibility using remotely sensed normalized difference vegetation index and the forecasted changes in the future, Science of The Total Environment, 770, 145288. https://doi.org/10.1016/j.scitotenv.2021.145288.

Varra, G., R. Della Morte, M. Tartaglia, A. Fiduccia, A. Zammuto, I. Agostino, C. A. Booth, N. Quinn, J. E. Lamond and L. Cozzolino, 2024. Flood Susceptibility Assessment for Improving the Resilience Capacity of Railway Infrastructure Networks. Water, 16(18), *2592.* https://doi.org/10.3390/w16182592

Vojtek, M., and J. Vojteková, 2019. Flood Susceptibility Mapping on a National Scale in Slovakia Using the Analytical Hierarchy Process. Water, 11(2), 364. https://doi.org/10.3390/w11020364

Yoo, C., E. Cho, W. Na, M. Kang and M. Lee, 2021. Change of rainfall–runoff processes in urban areas due to high-rise buildings, Journal of Hydrology. 597, 126155, https://doi.org/10.1016/j.jhydrol.2021.126155.